Proceedings of the Korean Nuclear Society Autumn Meeting
Taejon, Korea, October 2000

Critical Heat Flux of Water in Vertical Tubes with an upper Plenum and a Closed Bottom

Hong Chae Kim, Won Pil Baek and Soon Heung Chang

Korea Advanced Institute of Science and Technology
373-1 Kusung, Yusung
Taejon, Korea 305-701

Abstract

An experimental study is conducted for vertical round tubes with an upper plenum and a closed bottom to investigate CHF behavior and CHF onset location under the counter-current condition. The measured CHF values are well predicted by general Wallis type flooding correlations. A 1-D steady-state analytical flooding model for thermosyphon by El-Genk & Saber was assessed with the data and the liquid film thickness at the liquid entrance was calculated. The CHF onset position becomes different with *L/D* and *D*, and liquid entrance geometry affects only CHF values not CHF onset positions.

1. Introduction

There have been many experimental and theoretical works related to critical heat flux (CHF) as a limiting factor of heat transfer for the heat exchanging devices using change-of-phase phenomena. Nowadays, concerning accident analysis of nuclear reactors, CHF at accident condition (low pressure and low flow) also gets attention and some experimental works investigated CHF behavior and provided data bank. Besides the CHF phenomena at non-zero flow (low or high), CHF can occur at very low flow or zero flow with low heat flux. In some accident cases as loss-of-coolant accident or RCS depressurization, coolant flow is very low or even zero flow condition could be confronted. Khabensky et al. (1998) described some peculiarities and difficulties in CHF phenomena under zero coolant flow based on previous investigations;

(a) The heat transfer crisis mechanism in this case is different from the other boiling crisis mechanisms. It is necessary to match smoothly heat transfer crisis correlations at G=0 and |G|>0.
(b) The problem of localization of the crisis point and estimation of parameters in that moment; strong influence of the external circulation loop, structure peculiarities of test facility and channel geometry on the crisis phenomena.
(c) Scarcity of the test data bank for CHF for rod bundles with closed bottom.

In addition to nuclear reactors, CHF at zero-flow is interesting topic in some cases as vertical thermosyphon, heat pipes and steam generator in the boil-off condition under a loss-of-feedwater accident.

It is generally known that CHF mechanism at zero-flow is pool-boiling CHF in the tube of small length or large diameter and is flooding-limited CHF in long tubes. For nuclear reactor, the fact that cross sectional area of flow channel is small compared to the length of the channel (large *L/D*) suggest flooding phenomenon as the trigger of CHF. In a heated channel with a closed bottom, counter-current annular flow in which vapor flows upward and liquid film flows downward by gravity takes place. As heat flux increases, exit vapor flow gets higher velocity because of higher vapor generation and the interfacial shear force between vapor core and liquid film increases sufficiently to result in rapid growth of surface wave. At flooding condition, waves on the liquid film grow enough to bridge with the opposite side waves and finally the liquid film flow stops at the exit of the heated channel. The stoppage of the liquid flow into lower part of the heated channel results in dry-out of the thinnest liquid film at a place between channel exit and bottom. Because flooding occurs in complex fluid

geometry (waves, entrainment, bridge of waves, etc), the flooding phenomenon and flooding-limited CHF haven't been understood clearly by mechanistic model.

Many counter-current flow CHF experiments in vertical tubes with closed bottoms have been carried out mainly for the understanding of CHF in heat pipes and thermosyphons. Test section geometries largely can be classified into two types; closed two-phase thermosyphone consisting of heated section and cooled section, and vertical tube with a liquid reservoir and a closed bottom (Fig. 1). Most of the experiments were made with closed two-phase thermosyphon. However, CHF phenomenon in a vertical tube with a liquid reservoir and a closed bottom seems to be more similar to those in nuclear reactor at accident conditions. For this type of test section, relatively recent studies provided the following information.

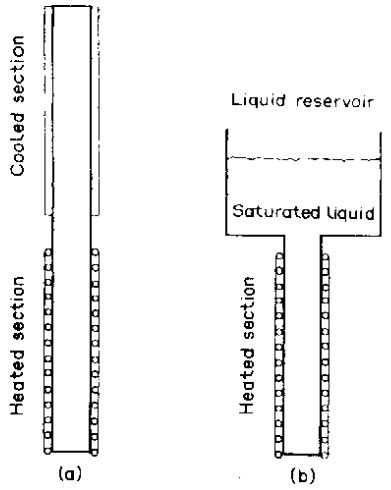

Fig. 1 (a) Closed two-phase thermosyphone. (b) Vertical tube with a liquid reservoir and a closed bottom

Barnard et al. (1974) measured CHF in tubes (D = 17.2 mm) using R-113 at atmospheric pressure ($\rho_v/\rho_l \approx (\rho_v/\rho_l)_{w,\,P=8.5\,bar}$) and observed the axial CHF onset position for various L/D conditions. From there investigation, Barnard et al. found that CHF onset position became closer to the bottom with the increase in heated length and suggested that in longer tubes (L/D > 70) CHF would be initiated at the bottom end in a flow condition where whole heated length were covered by liquid film and the liquid film thickness was thinnest at the bottom.

Nejat (1981) conducted CHF experiments with thee diameter of tubes (D = 8, 10, 14 mm) for relatively short heated section (L/D: 18.38, 15.00 and 10.71) using various liquid (water, carbon-tetrachloride, normal-hexane and ehtylalcohol) and investigated the effects of density ratio of liquid substance and length to diameter ratio on CHF. Nejat observed that the dry-out or burn-out condition due to the flooding mechanism is reached at the lower end of the tube when the flow of fluid into the tube from upper reservoir is controlled by the upward flow of its vapor and described that the flooding control occurs at the top end of the tube where the maximum flow rate of liquid and its vapor are involved and the heat flow rate would be equal to the total amount of heat supplied to the tube. He showed Wallis correlation was in good agreement with the experimental test data and the density ratio of liquid is an important parameter and suggested that the length to diameter ratio has an effect on the critical heat flux when 10.71 < L/D <35.21 and should be included in the correlation.

Smirnov (1984) performed experimental studies with electrically heated pipes with I.D. of 6, 9.2, 16 and 23 mm and with lengths ranging between 0.46 and 2.4 m. He also worked with annuli, consisting of concentric, 2.4 m long tubes with diameters of 23/12 and 23/18 mm, and also with seven-rod bundles (in which the tubes were arranged on an equilateral-triangle pattern). According to his observation, for the specific experimental conditions the "front" of decrease in heat transfer coefficient (DNB) travels toward the bottom end of the channel; when the power supplied to the channel is increased beyond critical power, the DNB region extends toward the top end of the channel. Departure from nucleate boiling in pipes was observed only in the bottom third of the pipe, whereas for rod

bundles it started in the second (from the top) quarter heated part of the channel length. He assumed the difference was most probably due to radial mass transfer between the individual subchannels in the rod bundles.

Recently, Katto and Hirao (1991) conducted experimental work using vertical tube (8, 10 mm) with a liquid reservoir (height of 150, 350 mm) and observed the effect of length to diameter effect on axial CHF onset position. From their observation of CHF onset position, they suggested a CHF occurrence model for zero flow. According to their study, presumption of Barnard et al. for CHF to arise at the bottom end of a heated tube if the tube is sufficiently long, is unrealized up to L/D = 125. The effect of the liquid level in the reservoir on CHF is negligibly small within the experimental range at least. Katto and Hirao represented their data and Barnard et al.'s data in generalized form using the relative distance of the CHF onset point measured from the bottom (Fig. 2 (a) and (b)). Recent experimental studies were listed in Table 1.

In the previous experimental works, there are still no agreements on the location of CHF onset and few CHF data for long tubes concerning CHF onset position. This experimental work was performed to get CHF data for tubes with a closed bottom and to investigate CHF behaviors; tube exit geometry effect on CHF and axial position of CHF onset with *L/D*.

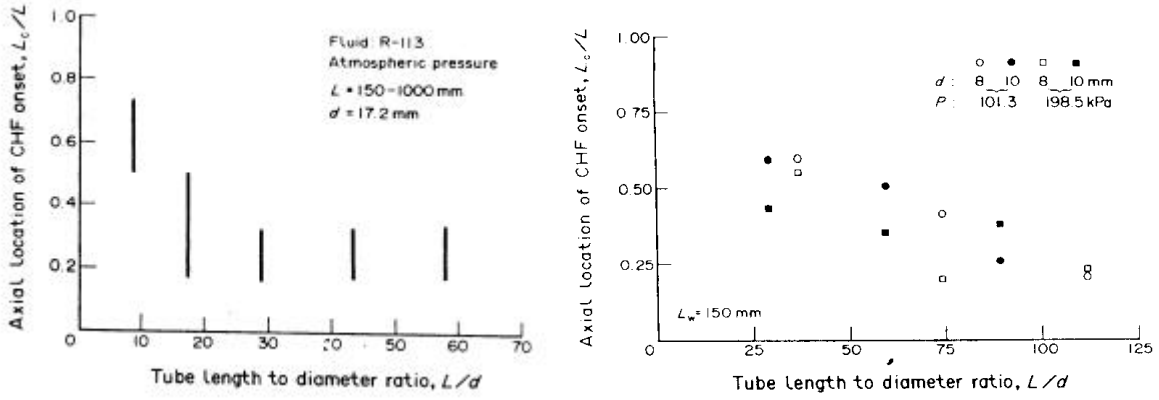

Fig. 2 Location of CHF onset ((a) Barnard et al. , (b) Katto and Hirao)

Table 1. CHF experiments of counter-current flow in a vertical tube with a reservoir and a closed bottom

Authors	Fluid	Test Section	Heating	D(mm)	L/D	P (MPa)	CHF onset location
Barnard et al. (1974)	R-113	Tube (Stainless steel)	Direct a.c.	17.2	8.7 – 58.1	0.1 r_v / r_l = 0.00495	Fig. 2 (a)
Nejat (1981)	Water C-T Hexane Ethylalcohol	Tube (Copper)	Electrical heating wire	8.0 – 14.0	10.7 – 18.4		
Smirnov (1984)	Water	Tube Annulus Rod-bundle	Electrical	6.0 –23.0	20.0 – 400.0	0.2 -12	Tube: Bottom third
Katto & Hirao (1991)	Water	Stainless steel	Direct a.c.	8.0 – 10.0	30.0 – 112.5		Fig. 2 (b)

2. Experiments

The experimental apparatus consisting of an upper liquid reservoir, a test-tube, a heater, and a measuring system for temperature and pressure was installed as illustrated in Fig.3.

The test section was made with Inconel-625 tube whose electrical and mechanical properties are well known and all of the test-tube have a wall thickness of 1mm except a tube 12 mm in inner diameter with a thickness of 1.5 mm. Both ends of the test section were connected to direct current power supply with clamp type electrodes and the test tube was heated uniformly with direct Joule heat. Chromel-alumel thermocouples were spot welded on the outer surface of the tube with equal interval (30 mm) to investigate the behavior of the temperature at each point and to observe the axial position of CHF onset during experiments.

The upper liquid reservoir with inner diameter of 265 mm and height of 500 mm was connected to the exit of the test tube using a changeable socket made for experiment with various liquid inlet conditions. The temperature of the reservoir water was kept constant, saturation temperature, using coil type heater (2kW) submerged in it and the level of the water could be checked with transparent level gauge during experiments. The changeable socket, made by stainless steel, was tapered with specific angle to investigate the effect of geometry of liquid inlet.

Experiments were performed with pure water and the water degassed before experiments by heating it with heater in reservoir and test section about 1 hour. Temperature and pressure of the reservoir were measured with thermocouple and pressure gauge put in reservoir pool.

The experiments were initiated by setting the level of the reservoir water and heating the water up to saturation condition. The voltage of the test section increased step by step with enough duration for the thermal equivalent of the water in the apparatus. CHF condition was defined as a sudden increase in the temperature of the tube surface and CHF onset position was considered as a point where the first temperature jump took place.

All of the experiments were performed at atmospheric condition with four diameters of tubes (6, 8, 10, 12 mm) for various heated length to diameter conditions (*L/D*: 25 ~ 300). The water level of the reservoir was kept 150 mm and the entrance angle varied from 0 ~ 90 °(Fig. 4).

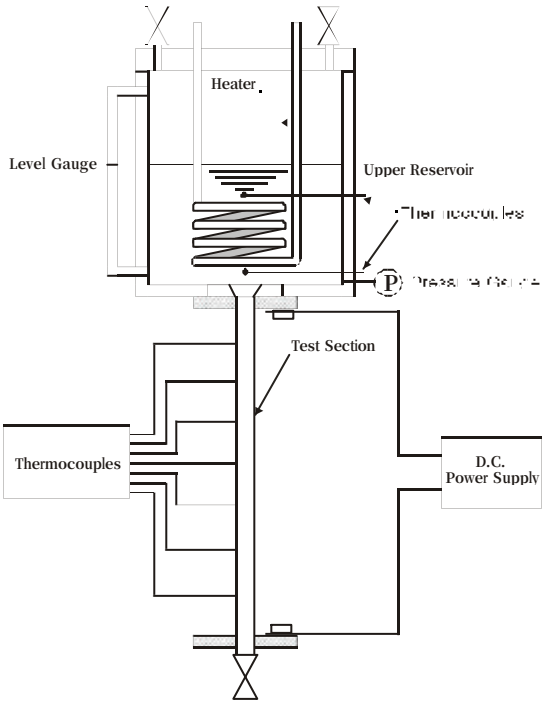

Fig 3. Experimental apparaus

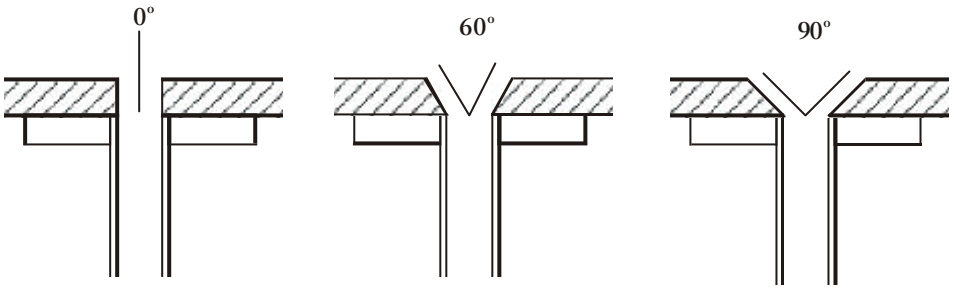

Fig. 4 Liquid entrance conditions of the experiment

3. Experimental Results

3.1 Behavior of the wall temperature

Temperature behaviors on the outer surfaces of the test tube give indirect information of tube internal boiling process and crisis at each axial position. Different from the cases of flow CHF where temperature suddenly increases at tube exit, temperature fluctuated periodically or increases gradually with time and the first jump of temperature took place at various points between tube exit and bottom for various heated length to diameter conditions. Fig. 5 (a) and (b) show the behavior of local wall temperature with time at some locations near CHF onset position, where *z* means a distance between CHF onset position and the bottom of the test tube and L means whole heated length of the tube. As shown in Fig. 5, temperature varied with two types; (a) periodical sudden increase and (b) gradual increase with large interval. The trends are very similar to those of Katto and Hirao (1991) shown in Fig. 6. Until about 70 ~ 80 seconds before the onset of CHF, temperatures at all position are nearly same and keep constant values for both of the two cases. After that, wall temperatures fell gradually towards the saturation temperature, and then suddenly increased. In Fig. 5 (a), following a sudden jump of temperature at a point with width of 10 ~ 20 second at peak bottom, similar peaks took place with some time interval (10 ~ 30 seconds). However, in Fig. 5(b), peaks occur continuously with width over 50 second. In Fig. 5 (a) and (b), the height of the first peak is smaller than those of other peaks taking place later. However, it is considered that CHF occurred at the first temperature peak. From the temperature fluctuation, it seems that the boundary between liquid and vapor is very complex and even though CHF occur at a point where the liquid film thickness is thinnest, upper liquid film in the form of wave or crest rewet the heated surfaces periodically. In Fig. 5 (b), this rewetting phenomena take place more slowly resulting in boiling crisis at wider range. After a recovery of the liquid on heated surface at CHF onset point, the dry-out didn't occur at same place. In Fig. 5 (a), the first peak was observed at z/L=0.28 in the first group of peaks, however, in second peak group, temperature jumped at z/L=0.35 with higher maximum temperature. It suggests that CHF onset position should be defined as a band with some width at a given experimental condition.

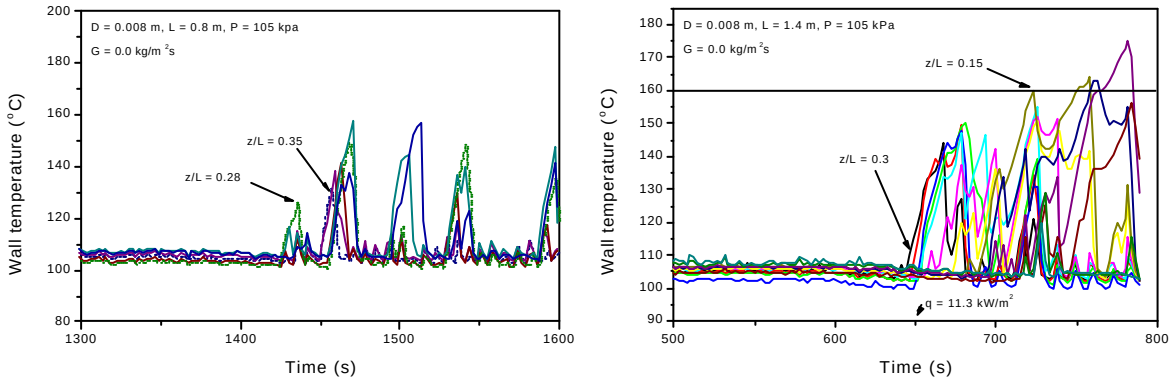

(a) (b)

Fig 5. Wall temperaure behavior

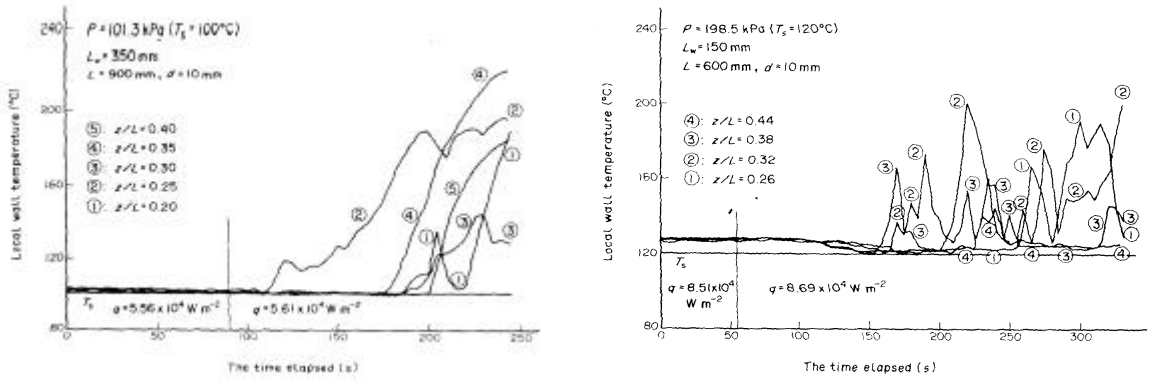

Fig 6. Wall temperaure behavior (Katto and Hirao, 1991)

3.2 CHF characteristics with *L/D*

Heat flux at which temperature changes abruptly in first with large difference is considered as CHF. In Fig. 7, the measured CHF values are plotted with *L/D* for 6 and 8 mm tubes. CHF decreases with increase in heated length and decrease rate become small for long tube. In the figure, some entrance effect was shown. The CHF values for the case of 0° are smaller than those for 60° and 90° regardless of the *L/D* value. This could be explained by effective diameter of vapor core at the entrance of upper liquid. In case of sharp edge, 0°, the liquid flows into the test section from the radial direction of the bottom of the upper plenum, which makes large wave at the entrance resulting in small flow area of vapor flow coming out of the test section. As the effective flow area of vapor steam becomes smaller, the friction between the vapor core and the liquid film become larger because of higher vapor velocity. Then, the stoppage of the liquid film could occur at lower heat flux and CHF values become lower.

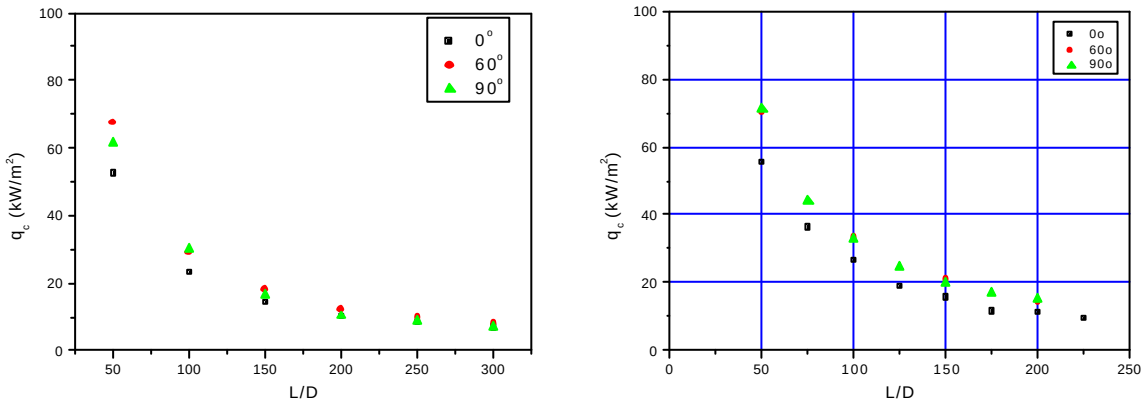

(a) 6 mm (b) 8 mm

Fig. 7 Characteristics of CHF

Some typical empirical flooding correlations, Wallis (1961), Tien & Chung (1979), Nejat (1981), Imura et al. (1983) and Baek et al. (1987), were compared with the data as shown in Fig. 8. All of the correlations have similar CHF trend with the data, however, the Wallis (1961) and Baek et al. (1987) correlations predict CHF much lower and higher than the measured value, respectively. In case of sharp entrance edge, Tien & Chung (1979) correlation well predicts the CHF and in case of smooth edge, 60° and 90°, Imura et al. (1983) does.

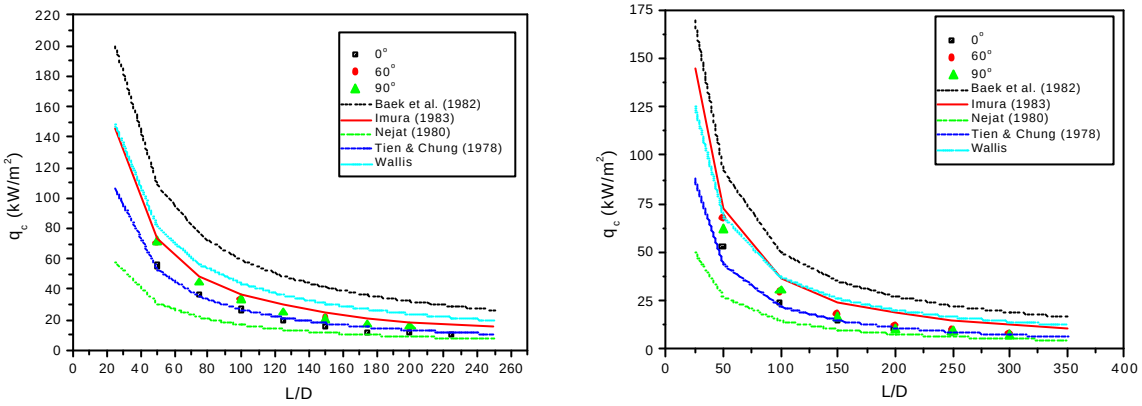

(a) 6 mm (b) 8 mm

Fig. 8 Comparison of the flooding correlations with the data

Related to the thermosyphons analysis, several analytical models have been developed. Among them, El-Genk & Saber (1997) suggested a one-dimensional, steady-state analytical model to predict the CCFL, which treats the shear at the liquid-vapor interface as the sum of two terms: (a) adiabatic shear stress; and (b) dynamic shear stress. The model predictions of wall film thickness were in good agreement (within ± 10%) with the data of other investigators for water and methanol. The basic assumptions incorporated in the model are;

(a) Axial pressure drop in the film is negligible,
(b) Effect of liquid droplets entrainment in vapor flow is negligible, and
(c) Average vapor flow velocity is equal to that at the vapor-film interface.

In case of water, the liquid film Reynolds number is generally smaller than 3500 at atmospheric pressure. So laminar liquid film flow model could be applied for the analysis (Fig. 9).

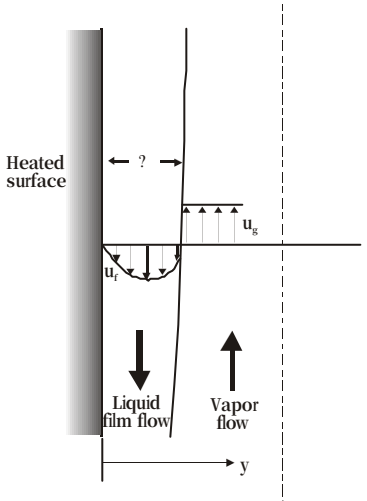

Fig. 9 Liquid and vapor flow model.

By solving the momentum balance equation for laminar flow film, radial velocity distribution of the liquid could be obtained as

$$u_f = \left(\frac{(r_f - r_g) g d - t_i}{m_f} \right) y - \left(\frac{(r_f - r_g) g}{2 m_f} \right) y^2 \qquad (1)$$

Integration of the velocity profile from the wall to the interface gives the average velocity of the liquid film.

$$\bar{u}_f = \left(\frac{(r_f - r_g)g}{3m_f} \right) d^2 - \left(\frac{t_i}{2m_f} \right) d \qquad (2)$$

The interfacial shear between the vapor core and the liquid film can be generally expressed as:

$$t_i = t_{ia} - t_{id} = t_{ia} - (u_i + u_g) \left(\frac{dW_g}{dx} \right) \qquad (3)$$

where, t_{ia} and W_g are the adiabatic shear and the amount of the vapor generation, respectively.
The average liquid film thickness at the liquid entrance also can be calculated with steady-state mass conservation equation.

$$\bar{u}_f = Q/(p(D-d)dh_{fg} r_f) \qquad (4)$$

By equating the equations (2) and (4), and substituting the interfacial shear with the equation (3), the liquid film thickness at the liquid entrance can be calculated. Figure 10 shows the definition of flooding condition in the analysis. As the wall heat flux increases, the liquid film thickness at the liquid entrance also increases because of increased interfacial shear. Over some heat flux, more increase of heat flux doesn't result larger liquid film thickness, but result smaller film thickness. At that condition, the heat flux is flooding heat flux and liquid film stops.

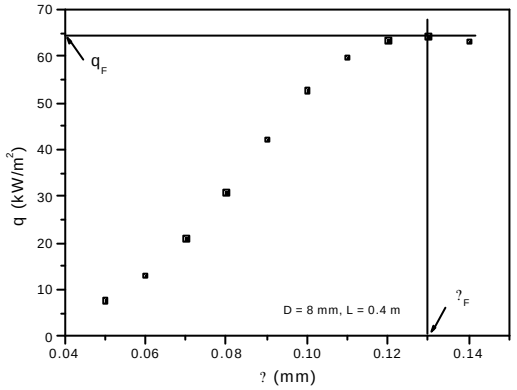

Fig. 10 Liquid film thickness trend with heat flux

The flooding heat fluxes predicted by El-Genk & Saber (1997)'s model are plotted with the experimental data in Fig. 11. The model shows good agreement with the data at all *L/D* conditions. All predicted values are within the measured values for 0º and 90º. Based on the accuracy of the model for the flooding heat flux with the data and liquid film thickness (El-Genk & Saber, 1997), the liquid film thickness at the liquid entrance (vapor exit) in case of flooding can be indirectly considered.

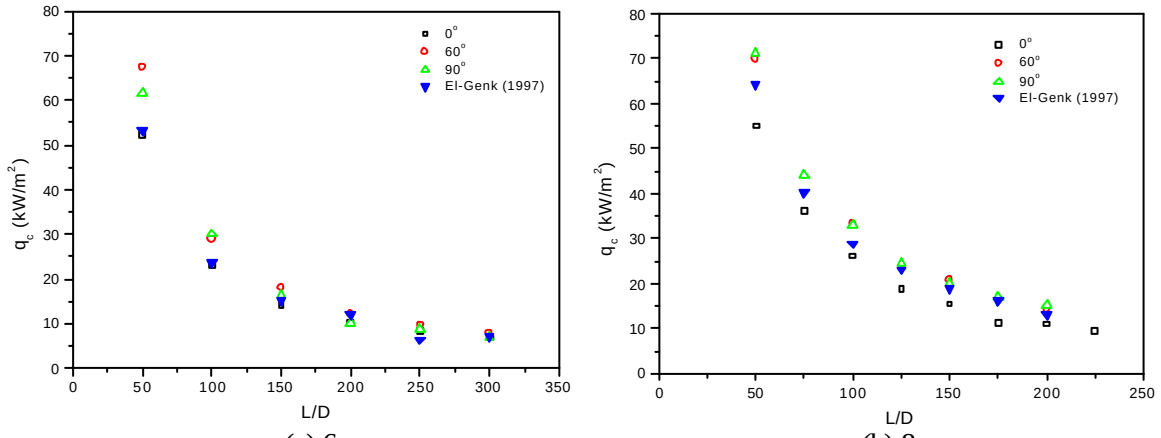

(a) 6 mm (b) 8 mm

Fig. 11 Comparison of the predictions by El-Genk & Saber model with the data

Figure 12 shows the liquid film thickness for 6 and 8 mm tubes at flooding heat flux. In larger diameter tube, flooding occurs with lager liquid film thickness. The liquid film thickness at flooding doesn't seem to depend on the *L/D* value. It means that the liquid film thickness is only the function of total power given to the whole test section.

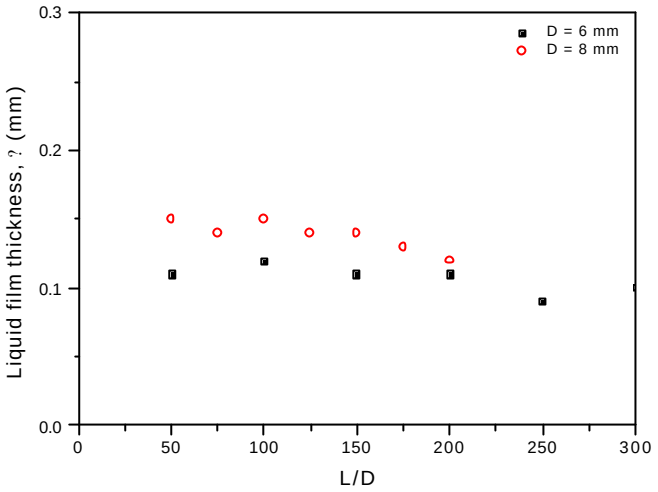

Fig. 12 Liquid film thickness at flooding heat flux

3.3 CHF onset position

In the present study, CHF onset position was defined as a point where the first wall temperature jump takes place and depicted as a fraction L_c/L, where L_c means distance between the CHF onset position and the bottom of the test tube and L means total heated length. Figure. 13 (a) shows the variation of CHF location for 6 mm tube with heated length to diameter. It should be noticed that the data have some uncertainty because of the thermocouples position which has interval of 30 mm between each of them. In the figure, the CHF onset position lies between L_c/L=0.1 and L_c/L=0.25. For 8 mm tube (Fig. 13 (b)), CHF onset position shows clear dependency on L/D. The trend is similar to those of Barnard et al. and Katto and Hirao. The data from Katto and Hirao are also platted in the figure for comparison. Katto and Hirao's experiments are for relatively short tubes ($L/D \leq 125$) and their data showed generally linear decreasing trend towards to bottom end of tube. According to their data, it seems that CHF would occur at tube bottom for tube of $L/D \approx 150$. In addition to that, Barnard et al. presumed that CHF arise at the bottom end of a heated tube if the tube is sufficiently long. However, in the present study, CHF occurred at a nearly constant position ($L_c/L \approx 0.25$) for long tubes ($L/D \geq 125$) and even at L/D = 200 CHF didn't take place at tube bottom.

Hwang and Chang developed a physical model for the prediction of dryout locations in a boiling channel with a closed bottom end on the basis of the liquid film dryout model and the two-phase mixture level theory. They assumed that the first dryout occurs at the boundary between the two-phase mixture region and the countercurrent annular flow region in the present boiling system. With their model, they calculated initial mixture level indicating the two-phase mixture level at the onset of flooding and final mixture level which is the mixture level when dryout occurs. Recently, Park et al. improved Hwang and Chang's model to take into account entrainments from the liquid film and to extend the applicable range to subcooled inlet flow conditions. For the calculation of the CHF, Wallis flooding correlation with newly proposed C_w^2 by them as a function of L/D, pressure and Bond number was used. In this study, Imura et al. (1983) and Tien & Chung (1979) correlations are used for the model because of their accuracy for the data. Predictions by the modified model are plotted in Fig. 13 (b) as a solid line. The predictions by the model are not in good agreement with the data. It seems that over the L/D = 125, CHF onset mechanism become different compared to the small L/D condition. In overall, the liquid entrance condition seems to have no affect on the CHF onset position.

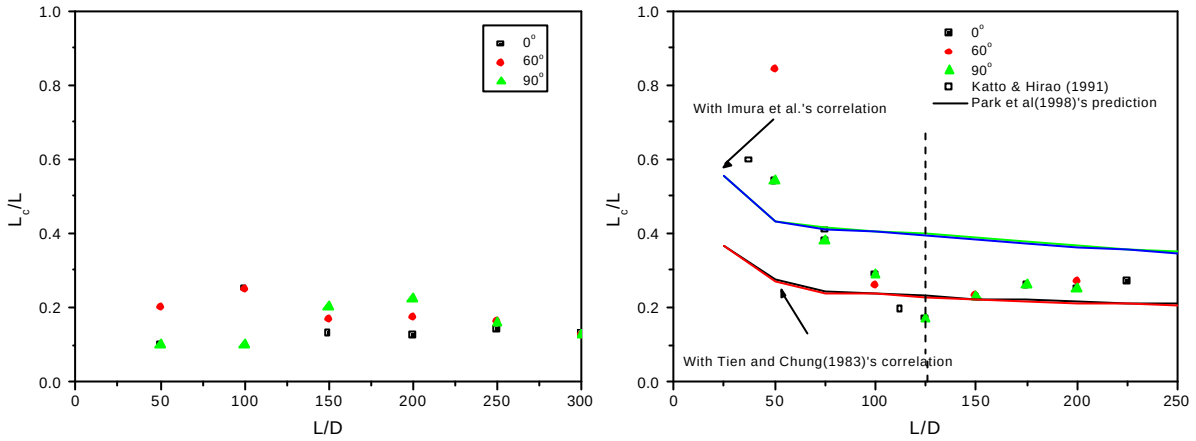

(a) 6 mm (b) 8 mm

Fig. 13 CHF onset position

4. Conclusions

Experiments of CHF for uniformly heated tubes with closed bottoms were performed for various *L/D* conditions in the existence of large upper reservoir to investigate the behavior of CHF onset position with *L/D*, to observe the end geometry effect of tube on CHF and to enlarge CHF data base. The reservoir was kept at saturation condition of atmospheric pressure through the experiments. From the analysis of the data and the observation of the wall temperature variation, the following conclusions can be made.

1. From the behavior of the wall temperature of the test section showing periodic rise with small or large time interval, periodic rewetting of dryout region with wave of liquid film seems to take place.
2. Tube inner diameter effect doesn't appear for a fixed *L/D* except at short tube and Imura et al.'s and Tien & Chung's correlations, a typical flooding correlations, show good agreement with the data.
3. General 1-D steady-state flooding analytical model (El-Genk and Saber) predict the CHF data well. According to the analysis with the model, liquid film thickness at flooding becomes larger with the increase of the inner tube diameter.
4. The locations of CHF onset shows different trend with diameter. In case of small diameter (D = 6 mm), CHF takes place at nearly same L_c/L. In case of 8 mm tube, two different trend regions appeared. For long tubes (L/D > 125), CHF occurs at nearly same L_c/L (=0.25), however, for short tubes (L/D <125), CHF onset position became smaller with the increase of L/D.
5. The geometry of the liquid entrance affects the CHF value. However, CHF onset positions were not affected by the entrance angle.

References

Barnard, D.A., Dell, F.R. and Stinchcombe, R.A., Dryout at low mass velocities for an upward boiling flow of Refrigerand-113 in a vertical tube, UKAEA, AERER, 7726, 1974.

El-Genk, M.S. and Saber, H.H., Flooding Limit in Closed, Two-Phase Flow Thermosyphon, *Int. J. Heat Mass Transfer*, Vol. 40, No. 9, 2147-2164, 1997.

Hwang, D.H. and Chang S.H., Development of a Phenomenological Model for the Prediction of Dryout Locations under Flooding-Limited Critical Heat Flux Conditions, *Nucl. Eng. Des.*, Vol. 148, 475-486, 1994.

Imura, H., Sasaguchi, K. and Kozai, H., Critical Heat Flux in a Closed Two-Phase Thermosyphon, *Int. J. Heat Mass Transfer*, Vol. 26, No. 8, 1181-1188, 1983.

Katto, Y. and Hirao, T., Critical Heat Flux of Counter-Flow Boiling in a Uniformly Heated Vertical Tube with a Closed Bottom, *Int. J. Heat Mass Transfer*, Vol. 34, No. 4/5, 993-1001, 1991.

Khabensky, V.B., Malkin, S.D., Shalia, V.V., Ilukhin, Y.N. and Nigmatulin, B.I., Critical Heat Flux Prediction in Vertical Bottom-Closed Rod Bundles, *Nucl. Eng. Des.*, Vol. 182, 203-224, 1998.

Nejat, Z., Effect of Density Ratio on Critical Heat Flux in Closed End Vertical Tubes, *Int. J. Multiphase Flow*, Vol. 7, 321-327, 1981

Park, C. Chang, Hwang, D.H, Chang, S.H. and Won Pil Baek, An improved physical model for flooding-limited CHF at zero and very low flow conditions, *Int. Comm. Heat Mass Transfer*, 1998.

Smirnov, Y.L., Critical Heat Flux in Flooding in Vertical Channels, *Heat Transfer-Soviet Research*, Vol. 16, No. 3, 19-24, 1984.

Tien C.L. and Chung, K.S., Entrainment Limits in Heat Pipes, *AIAA Journal*, Vol.17, No. 6, 643-646, 1979